Communication capacity of a free space laser communication system in atmospheric turbulent and disperse channels

Hongqiang Lu (陆红强)[1,2*], Wei Zhao (赵 卫)[1], and Xiaoping Xie (谢小平)[1,3]

[1]*State Key Laboratory of Transient Optics and Photonics, Xi'an Institute of Optics and Precision Mechanics, Chinese Academy of Sciences, Xi'an 710119, China*

[2]*Graduate University of Chinese Academy of Sciences, Beijing 100049, China*

[3]*Xi'an Communication College, Xi'an 710106, China*

[*]*Corresponding author: luhongqiang@opt.ac.cn or lhq555@gmail.com*

Received December 21, 2010; accepted January 30, 2011; posted online June 27, 2011

The pulse broadening and communication capacity in atmospheric turbulent and disperse channels are investigated. Models on pulse broadening are proposed, and the simulated results for a typical atmospheric condition and configuration are provided. The results show that the capacity of the system is affected mainly by atmospheric dispersion rather than atmospheric turbulence. The received pulse width can be minimized, and the system-achievable capacity can be maximized by selecting the optimum input pulse width. The proposed method can be used to predict the achievable capacity of a free space laser communication system in turbulent and disperse channels.

OCIS codes: 060.2605, 010.3310, 010.1300.

doi: 10.3788/COL201109.S10603.

Free space laser communication systems, which use the atmosphere as a propagation medium, have attracted much attention during the last two or three decades. Optical waves have a high frequency, and they have many advantages compared with radio frequency, such as high data transmission rate[1]. In the last decade, the single-channel capacity of free space laser communication systems has increased from 10 to 160 Gb/s[2−4]. To the best of our knowledge, the highest transmission rate of a single channel was 1.28 Tb/s in the optical time division multiplexing system, which was demonstrated in 2000[5]. In the optical transmitting channel, optical pulse signals undergo atmospheric turbulence[6−10], atmospheric dispersion, and so on[11], which in turn cause pulse broadening and consequently limit the available capacity of the channel. However, pulse broadening, especially dispersion-induced pulse broadening, in a free space laser communication system has received little attention in the previous related literature. The possible reason is that the available free space laser communication operates at a relatively low data rate and short transmitting distance. With the increment in communication capacity (narrower pulse width) and transmitting distance, the temporal broadening of an optical signal must be taken into consideration.

The temporal broadening of a pulse through a random medium is caused primarily by two mechanisms, the scattering process of the medium and the wandering of the pulse[6]. Pulse temporal broadening can be deduced from knowledge on the two-frequency mutual coherence function[7]. The input waveform is attributed to the Gaussian pulse and can be described by

$$v_i(t) = A\exp(-t^2/T_0^2), \tag{1}$$

where A and T_0 are the amplitude and the width of the Gaussian pulse, respectively. The mean irradiance of the received pulse located at distance L from the transmitter is given by[8]

$$\begin{aligned}\langle I(r,L;t)\rangle \approx &\Big(\frac{W_0}{2Lc}\Big)^2\frac{T_0^2[T_0^2(1+w_0^2T_0^2)+(W_0r/Lc)^2]}{T_n[T_0^2+(W_0r/Lc)^2]^{5/2}}\\ &\times\exp\Big\{-\frac{(w_0T_0W_0r/Lc)^2}{2[T_0^2+(W_0r/Lc)^2]}\Big\}\\ &\times\exp\Big\{-\frac{2(t-L/c-r^2/2Lc)^2}{T_n^2}\Big\},\end{aligned} \tag{2}$$

where w_0 is the carrier frequency of the modulated signal, r is the vector in the transverse plane at propagation distance L, W_0 is the beam radius at the transmitter, c is the speed of light in vacuum, and T_n is the width of a turbulence-induced pulse at the receiver, which can be written as

$$T_n = \sqrt{T_0^2+8a} \quad , \tag{3}$$

where

$$a = \frac{0.391(1+0.171\delta^2-0.287\delta^{5/3})\mu_1\sec(\xi)}{c^2}. \tag{4}$$

Here inner scale ($l_0 = \delta L_0(h)$) and outer scale ($L_0(h)$) effects have been taken into account. ξ is the zenith angle, and μ_1 is an integral with respect to altitude

$$\mu_1 = \int_{h_0}^{h_f} C_n^2(h)[L_0(h)^{5/3}], \tag{5}$$

where h_0 is the altitude of the transmitter, h_f is the altitude of the receiver, $C_n^2(h)$ is given as

$$\begin{aligned}C_n^2(h) = \ &0.00594\Big(\frac{v}{27}\Big)^2(10^{-5}h)^{10}\exp(-h/1000)\\ &+2.7\times10^{-16}\exp(-h/1500)\\ &+B\exp(-h/100),\end{aligned} \tag{6}$$

where v is the pseudo wind in meters/second, and B is the nominal value of $C_n^2(h)$ at the earth's surface in $\mathrm{m}^{-2/3}$.

The turbulence-induced pulse broadening becomes negligible for the initial pulse width T_0 larger than 20 fs[8]. This is due to the pulse width in free space laser communication systems is not less than several picoseconds. The turbulence-induced pulse broadening is neglected.

The index of refraction n is one of the most significant parameters of the atmosphere for optical wave propagation, which is sensitive to fluctuations in temperature and pressure. The index of refraction of the atmosphere can be expressed as follows for optical and infrared wavelengths[12]

$$n = 1 + 77.6(1 + 7.52 \times 10^{-3}\lambda^{-2})\frac{P}{T} \times 10^{-6}, \qquad (7)$$

where λ is the optical wavelength in μm, P is the pressure in millibars (1 millibars = 100 Pa), and T is the absolute temperature in Kelvin. Temperature and pressure change with the altitude and the measured data in Xinjiang, China, are used in our simulation[13]. Propagation constant β can be expressed as

$$\begin{aligned}\beta(\omega) &= n(\omega)\frac{\omega}{c} \\ &= \frac{\omega}{c}\left(1 + 77.6\left(1 + 7.52 \times 10^{-15}\frac{\omega^2}{(2\pi v)^2}\right)\frac{P}{T} \times 10^{-4}\right) \\ &= \frac{\omega}{c} + 77.6\left(\frac{\omega}{c} + 7.52 \times 10^{-15}\frac{\omega^3}{(4\pi^2 v^2 c)}\right)\frac{P}{T} \times 10^{-4},\end{aligned} \qquad (8)$$

where ω is angular frequency ($\lambda = 2\pi v/\omega$), and v is the speed of light in the transmitting channel. The propagation constant is then expanded as a function of the frequency difference $\omega - \omega_0$ (ω_0 is the carrier frequency) in a four-terms Taylor series

$$\begin{aligned}\beta(\omega) &= n(\omega)\frac{\omega}{c} \\ &= \beta_0 + \beta_1(\omega - \omega_0) + \frac{1}{2}\beta_2(\omega - \omega_0)^2 + \frac{1}{6}\beta_3(\omega - \omega_0)^3,\end{aligned} \qquad (9)$$

where β_1, β_2, and β_3 are the derivatives of the propagation constant. Considering the effects of dispersion and chirp, the effects of β_3 on pulse broadening are neglected due to the small value of β_3 and the received pulse width in single-mode fibers are given as[14]

$$\frac{T_\mathrm{n}^2}{T_0^2} = \left(1 + \frac{C\beta_2 z}{T_0^2}\right)^2 + (1 + T_0^2 W^2)\frac{\beta_2^2 z^2}{T_0^4}, \qquad (10)$$

where C is the chirp parameter of the optical modulator, and W is the 1/e half width of the optical source spectrum. Equation (10) is used to calculate atmospheric dispersion-induced pulse broadening, and the main difference between the single-mode fiber and the atmospheric channel is the index of refraction n. The index of refraction of a single-mode fiber can be regarded as a constant. However, the index of refraction of the atmosphere changes with the altitude. Considering the fluctuations in the index of refraction and β_2 of the atmosphere, the whole propagation channel is divided into N independent segments with interval Δh to describe pulse broadening accurately. The index of refraction and β_2 are treated as constants in each interval. For a large N, we then have

$$\begin{aligned}\frac{T_{i+1}}{T_i} = &\left\{\left[1 + \frac{C\beta_2(i \times \Delta h) \times \Delta h}{T_\mathrm{i}^2\cos(\xi)}\right]^2\right. \\ &\left. + (1 + T_\mathrm{i}^2 W^2)\left[\frac{\beta_2(i \times \Delta h) \times \Delta h}{T_\mathrm{i}^2\cos(\xi)}\right]^2\right\}^{1/2}, \\ &i = 1, 2, \cdots N.\end{aligned} \qquad (11)$$

The broadening ratios (T_n/T_0) as a function of the zenith angle and input pulse width are shown in Fig. 1. Assuming the propagation height is 30 km, the optical wavelength λ is 1550 nm, the chirp parameter is 0.8, and the spectral width is 125 GHz. The pulse broadening is very significant when the pulse width is in the order of 2 ps, and it is negligible if the pulse width is larger than 10 ps. Figure 2 shows the changes in broadening ratios with the input pulse width and propagating height. The broadening ratio increases with the input pulse width and propagating height. Due to the thin atmosphere and small dispersion parameter (β), the pulse broadening can be neglected when the propagation height is larger than 30 km.

The pulse width in free space laser communication systems is not less than several picoseconds, so turbulence-induced pulse broadening is neglected. The received

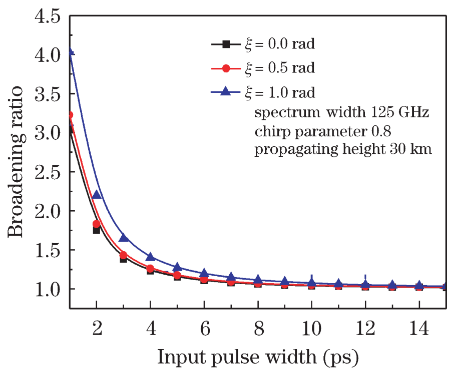

Fig. 1. Broadening ratios as a function of input pulse width for various zenith angles.

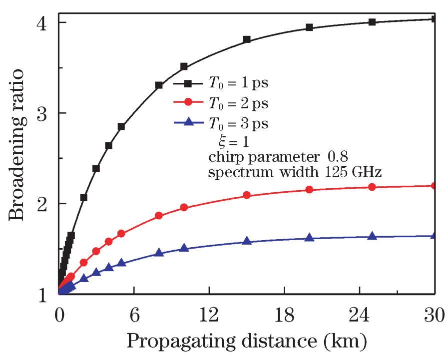

Fig. 2. Broadening ratios as a function of propagating height for various input pulse widths.

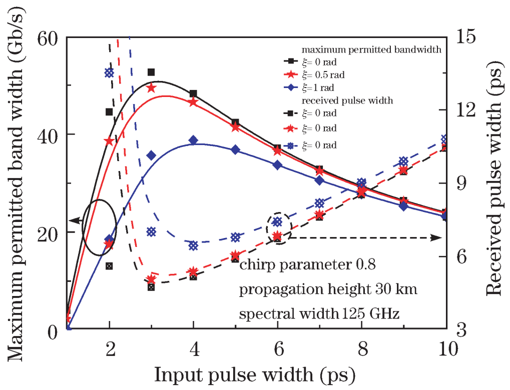

Fig. 3. Received pulse width and achievable capacity as a function of input pulse width for various zenith angles.

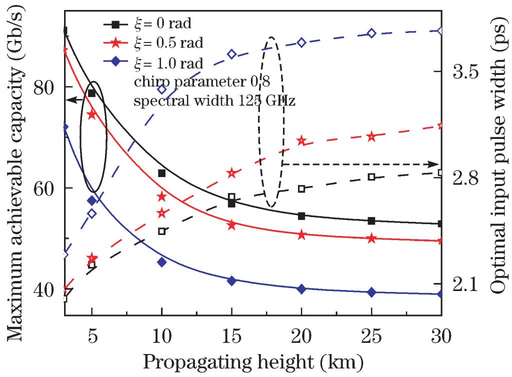

Fig. 4. T_{opt} and B_{max} as a function of propagating height for various zenith angles.

pulse width is attributed to the original pulse width and broadening ratio, and a smaller original input pulse width corresponds to a larger broadening ratio. Considering their combined effect, there should be a minimum received pulse width that can meet the maximum achievable communication capacity. The variation in received pulse width as a function of the input pulse width at various zenith angles is shown in Fig. 3. The existence of the minimum received pulse width can be clearly seen in all three curves. With the increment in zenith angles, the input pulse width corresponding to the minimum received pulse width skews toward larger values.

Evidently, dispersion-induced pulse broadening leads to a reduction in capacity, and a quantitative description of this reduction is used. The broadened pulse width T_n and the achievable capacity B can be related using the criterion that the broadened pulse should remain confined to its bit slot ($B = 1/T_p$, where T_p is the bit slot), and the achievable capacity is obtained using $4T_n$B < 1[15]. The curves of the maximum achievable capacity are also shown in Fig. 3, which correspond to the received pulse width. The maximum capacity decreases as the zenith angle increases.

Corresponding to the minimum received pulse width, there should be a optimum input pulse width, T_{opt}, which is derived by

$$\left.\frac{\partial T_n}{\partial T_0}\right|_{H,\xi} = 0, \quad (12)$$

where T_0 is the variation. This equation is solved numerically, and the results are given in Fig. 4. T_{opt} increases with the propagating height and the zenith angle. For instance, at $H = 5$ km, T_{opt} is 2.224 ps for $\xi = 0$ rad, 2.269 ps for $\xi = 0.5$ rad, and 2.563 ps for $\xi = 1$ rad.

In addition, there should also be a maximum capacity, B_{max}, which can be derived by

$$B_{max} = \frac{1}{4T_{opt}}. \quad (13)$$

In Fig. 4, the maximum capacity B_{max} decreases with increase in the zenith angle and propagating height.

In conclusion, the pulse broadening and communication capacity in optical turbulent and disperse channels have been investigated. The formulas for turbulence-induced pulse broadening are introduced, and a model on dispersion-induced pulse broadening is proposed. The results show that the capacity of the system is affected mainly by atmospheric dispersion. The received pulse width can be minimized, and the system-achievable capacity can be maximized by selecting the optimum input pulse width. This optimum input pulse width increases with the propagating height and zenith angle, and the maximum achievable capacity decreases with the propagating height and zenith angle. The method in this letter can be used to predict the available capacity of a free space laser communication system in turbulent and disperse channels, and the simulation results presented are reasonable. These findings should be highly considered in high-speed and long-distance free space laser communication systems. Further investigations, including experimental measurements based on optical time-division multiplexing technology, are being undertaken.

This work was supported by the National High technology Research and Development Program.

References

1. M. Toyoshima, J. Opt. Networking **4,** 300 (2005).
2. D.-Y. Song, Y.-S. Hurh, J.-W. Cho, J.-H. Lim, D.-W. Lee, J.-S. Lee, and Y. Chung, Opt. Express **7,** 280 (2000).
3. E. Ciaramella, Y. Arimoto, G. Contestabile, M. Presi, A. D. Errico, and M. Matsumoto, in *Proceedings of OFC2009* OMN7 (2009).
4. G. Nykolak, G. Raybon, B. Mikkelsen, B. B. Brown, P. F. Szajowski, J. J. Auborn, and H. M. Presby, Proc. SPIE **4214,** 11 (2001).
5. M. Nakazawa, T. Yamamoto, and K. R. Tamura, Electron. Lett. **36,** 2027 (2000).
6. C. H. Liu and K. C. Yeh, Radio Science **14,** 925 (1979).
7. C. Y. Young, A. Ishimaru, and L. C. Andrews, Appl. Opt. **35,** 6522 (1996).
8. D. E. Kelly, C. Y. Young, and L. C. Andrews, Proc. SPIE **3266,** 231 (1998).
9. M. Aharonovich and S. Arnon, J. Opt. Soc. Am. **22,** 1646 (2005).
10. R. Rao, Chin. Opt. Lett. **6,** 547 (2008).
11. T. Feng, G. Chen, and Z. Fang, Chin. Opt. Lett. **4,** 633 (2006).
12. H. Weichel, *Laser Beam Propagation in the Atmosphere* (SPIE, Washington, 1990).
13. Y. Han, X. Qiang, J. Feng, S. Liang, Y. Hu, and Y. Li, Infrared and laser Engineering (in Chinese) **38,** 267 (2009).
14. D. Marcuse, Appl. Opt. **20,** 3573 (1981).
15. G. P. Agrawal, *Nonlinear Fiber Optics* (Elsevier, Singapore, 2005).